



Universiteit
Leiden
The Netherlands

Synthesis and Characterization of Trinuclear [Ni₂Ru] Complexes with Bridging Thiolate or Selenolate Donors for Electrocatalytic Proton Reduction

Gezer, G.; Durán Jiménez, D.; Siegler, M.A.; Bouwman, E.

Citation

Gezer, G., Durán Jiménez, D., Siegler, M. A., & Bouwman, E. (2017). Synthesis and Characterization of Trinuclear [Ni₂Ru] Complexes with Bridging Thiolate or Selenolate Donors for Electrocatalytic Proton Reduction. *European Journal Of Inorganic Chemistry*, 2017(43), 5027-5032. doi:10.1002/ejic.201700941

Version: Not Applicable (or Unknown)

License: [Leiden University Non-exclusive license](#)

Downloaded from: <https://hdl.handle.net/1887/57424>

Note: To cite this publication please use the final published version (if applicable).

Se versus S in Hydrogenase Models

Synthesis and Characterization of Trinuclear [Ni₂Ru] Complexes with Bridging Thiolate or Selenolate Donors for Electrocatalytic Proton ReductionGamze Gezer,^[a] Dinesh Durán Jiménez,^[a] Maxime A. Siegler,^[b] and Elisabeth Bouwman*^[a]

Abstract: Two new trinuclear compounds $[[\text{Ni}(\text{x}b\text{SmS})]_2\text{Ru}(\text{phen})_2](\text{PF}_6)_2$ (**1**) and $[[\text{Ni}(\text{x}b\text{SmSe})]_2\text{Ru}(\text{phen})_2](\text{PF}_6)_2$ (**2**) were synthesized by the reaction of $[\text{Ni}(\text{x}b\text{SmS})]$ and $[\text{Ni}(\text{x}b\text{SmSe})]$, respectively, with *cis*- $[\text{Ru}(\text{phen})_2(\text{Cl})_2]$ [$\text{H}_2\text{x}b\text{SmS}$ = 1,2-bis(4-mercapto-3,3-dimethyl-2-thiabutyl)benzene; $\text{H}_2\text{x}b\text{SmSe}$ = 1,2-bis(2-thiabutyl-3,3-dimethyl-4-selenol)benzene; phen = phenanthroline]. The two $[\text{Ni}_2\text{Ru}]$ complexes were characterized by ESI-MS, NMR spectroscopy, elemental analysis, single-crystal X-ray crys-

tallography, and electrochemical techniques. X-ray structure determinations showed that the trinuclear complex cations in **1** and **2** contain two square-planar nickel centers bound in *cis* positions to the octahedral ruthenium ion by a bridging thiolate or selenolate donor atom. Electrocatalytic proton reduction occurs for both complexes in acetonitrile with the addition of varying amounts of acetic acid at a potential of -2.1 V vs. Fc^+/Fc with faradaic yields of around 65 %.

Introduction

Molecular hydrogen (H_2) is a perfect candidate as an energy carrier to be used as an alternative to fossil fuels. The hydrogen economy relies on the vision of replacing fossil fuels by dihydrogen as a low-carbon energy source.^[1] A way of producing dihydrogen gas is from the (electrocatalytic) hydrogen evolution reaction (HER), in which protons are combined with electrons to yield molecular hydrogen as shown in Equation (1):^[2]



In 1930 Stephenson and Stickland reported an enzyme found in certain microorganisms capable of molecular hydrogen activation for which they proposed the name hydrogenase.^[3] It was discovered that in microorganisms containing this hydrogenase dihydrogen can be produced or used as a source of electrons in a global H_2 cycle. The hydrogenase family is divided into three classes based on the identity of the metal ions at the active site, the $[\text{NiFe}]$, $[\text{FeFe}]$, and $[\text{Fe}]$ hydrogenases, which catalyze proton reduction or dihydrogen oxidation at very high rates.^[4] Many structural and functional models for the active site in $[\text{FeFe}]$ hydrogenase have been reported, but functional models of the $[\text{NiFe}]$ hydrogenases are less mature.^[5] In order to produce efficient functional models of the active site of $[\text{NiFe}]$ hydrogenases organometallic $[\text{NiFe}]$ and even $[\text{NiRu}]$ coordination compounds have been prepared.^[6] The choice for

ruthenium to replace iron in the design of functional mimics for the active site in $[\text{NiFe}]$ hydrogenases is based on the knowledge that ruthenium complexes are active as (homogeneous) catalysts in hydrogenation and hydrogen-transfer reactions and generally form more stable coordination compounds. Most significant is the fact that Ru^{II} ions are able to accept both soft and hard ligands such as dihydrogen and hydrides, which makes it suitable for replacing the Fe center in models of the $[\text{NiFe}]$ hydrogenases.^[6] In the past decade several heterodinuclear $[\text{NiRu}]$ complexes have been reported as structural and functional models of $[\text{NiFe}]$ hydrogenases.^[7–11] A subclass of $[\text{NiFe}]$ hydrogenases comprises the $[\text{NiFeSe}]$ hydrogenases, in which one of the non-bridging cysteines (Cys) in the active site of the enzyme is replaced by selenocysteine (Sec).^[12] Until now only a few studies have been directed to mimic the active site of $[\text{NiFeSe}]$ hydrogenase using a selenolate ligand coordinated to the nickel center.^[13,14]

The aim of this research is the synthesis and characterization of a novel electrocatalyst for the reduction of protons to dihydrogen gas. Previously, it has been shown that catalysts based on heterodinuclear $[\text{NiRu}]$ compounds are promising electrocatalysts for the HER.^[10] The introduction of large and bulky ligands for steric protection of the ruthenium center in the $[\text{NiRu}]$ -based catalysts has been reported to result in increased stability during the catalytic cycle.^[10] In this paper our study describes two new trinuclear $[\text{NiRu}]$ complexes derived from a reaction of the compounds $[\text{Ni}(\text{x}b\text{SmS})]$ ^[15] and $[\text{Ni}(\text{x}b\text{SmSe})]$ ^[13] with *cis*- $[\text{Ru}(\text{phen})_2(\text{Cl})_2]$ [$\text{H}_2\text{x}b\text{SmS}$ = 1,2-bis(4-mercapto-3,3-dimethyl-2-thiabutyl)benzene; $\text{H}_2\text{x}b\text{SmSe}$ = 1,2-bis(2-thiabutyl-3,3-dimethyl-4-selenol)benzene; phen = phenanthroline].^[16] Both NiS_4 and NiS_2Se_2 complexes are used in order to investigate the effect of changing the sulfur donor atom to selenium, inspired by the active sites in $[\text{NiFe}]$ and $[\text{NiFeSe}]$ hydrogenases. Generally, it is assumed that the Sec-

[a] Leiden Institute of Chemistry, Leiden University,
P. O. Box 9502, 2300 RA Leiden, The Netherlands
E-mail: bouwman@chem.leidenuniv.nl
<http://mcbim.lic.leidenuniv.nl/>

[b] Department of Chemistry, Johns Hopkins University,
21213 Maryland, U.S.A.

Supporting information and ORCID(s) from the author(s) for this article are available on the WWW under <https://doi.org/10.1002/ejic.201700941>.

containing redox proteins show higher catalytic activities than their Cys-containing homologues due to the different properties of selenium compared with sulfur, such as its higher nucleophilicity and acidity.^[13,17] The aim of the research described in this paper was to investigate whether such an enhanced catalytic activity caused by selenium donor atoms would also be found in model complexes.

Results

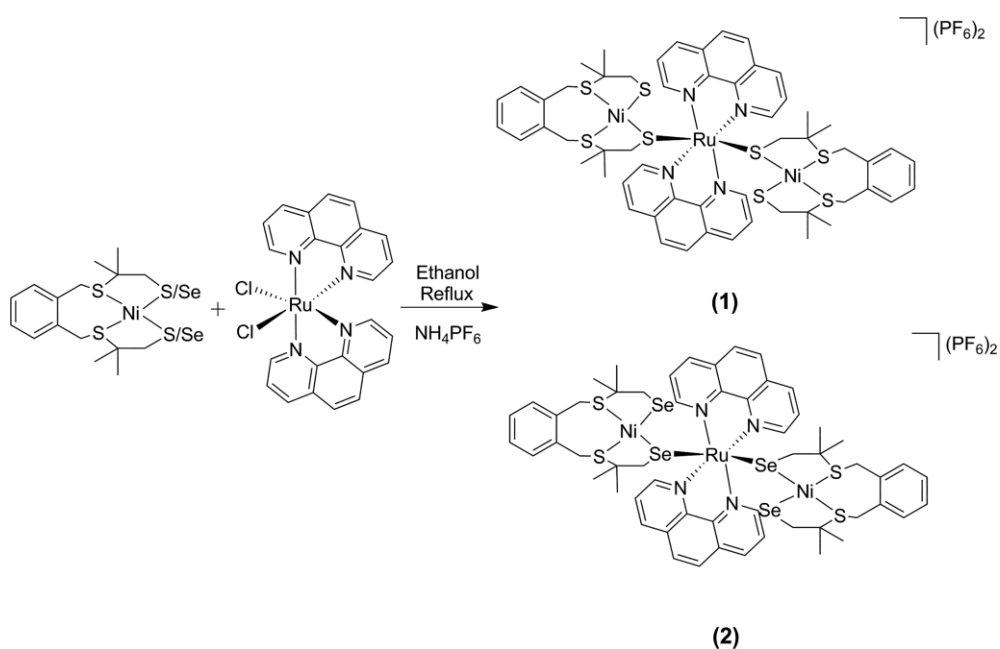
Synthesis and Characterization

The mononuclear nickel and ruthenium precursor complexes were synthesized according to reported procedures.^[13,15,16] The novel trinuclear complexes $[\{\text{Ni}(\text{x}b\text{SmS})\}_2\text{Ru}(\text{phen})_2](\text{PF}_6)_2$ (**1**) and $[\{\text{Ni}(\text{x}b\text{SmSe})\}_2\text{Ru}(\text{phen})_2](\text{PF}_6)_2$ (**2**) were synthesized by refluxing an ethanolic solution of $[\text{Ni}(\text{x}b\text{SmS})]$ or $[\text{Ni}(\text{x}b\text{SmSe})]$ with *cis*- $[\text{Ru}(\text{phen})_2(\text{Cl})_2]$ after which the chloride anions were exchanged with PF_6^- anions using NH_4PF_6 . The compounds were obtained as dark reddish-brown solids in 43 % and 46 % yield, respectively (Scheme 1). It was our intention to prepare dinuclear NiRu complexes with two bridging thiolates starting from a 1:1 ratio of the nickel and ruthenium complexes. However, the NMR spectra of the obtained complexes were not in agreement with the expected dinuclear compounds. The crystal structures of the obtained complexes surprisingly showed that trinuclear $[\text{Ni}_2\text{Ru}]$ complexes were obtained instead. The synthesis of the compounds was then optimized using a 2:1 ratio of the precursor nickel and ruthenium complexes. Both $[\text{Ni}_2\text{Ru}]$ complexes were characterized by ^1H NMR spectroscopy, mass spectrometry, elemental analysis, and single-crystal X-ray crystallography. Although acetone solutions of both complexes give rise to sharp resonances in the ^1H NMR spectra, it is difficult to assign all peaks in the aromatic region. The ESI mass spectra of the complexes exhibit the parent molecular ion peaks at

$m/z = 633.7$ and 727.2 for **1** and **2**, respectively, for the trinuclear dicationic compound $[\text{M} - 2 \text{PF}_6]^{2+}$.

Description of the Structures

Single crystals of the compounds $[\{\text{Ni}(\text{x}b\text{SmS})\}_2\text{Ru}(\text{phen})_2](\text{PF}_6)_2$ (**1**) and $[\{\text{Ni}(\text{x}b\text{SmSe})\}_2\text{Ru}(\text{phen})_2](\text{PF}_6)_2$ (**2**) were obtained by vapor diffusion of 2-propanol into acetone solutions of the complexes. Projections of the structures of **1** and **2** are given in Figure 1; selected interatomic distances and angles are provided in Table 1. For complex **1**, one of the two Ni units and one phenanthroline ligand coordinated to Ru are disordered over two orientations. The crystal structure also contains lattice acetone solvent molecules that together with the PF_6^- ions are disordered over two orientations. The crystal lattice of complex **2** also contains some amounts of lattice acetone solvent molecules and two PF_6^- ions disordered over two or three orientations. The trinuclear complex cations in **1** and **2** contain two square-planar nickel centers bound in *cis* positions to the octahedral ruthenium ion by a bridging thiolate or selenolate donor atom with S–Ru–S and Se–Ru–Se angles of $90.80(15)^\circ$ and $88.969(13)^\circ$, respectively. The square-planar coordination environment of the Ni^{II} centers comprises two thioether and two thiolate/selenolate donor atoms in mutual *cis* positions and is slightly distorted with dihedral angles of 12.17° and 16.9° , defined by the planes $\text{S}_{\text{thioether}}\text{--Ni--S}_{\text{thioether}}$ and $\text{S}_{\text{thiolate}}\text{--Ni--S}_{\text{thiolate}}$, respectively, for complex **1**, and 9.74° and 12.14° defined by the planes S–Ni–S and Se–Ni–Se, respectively, for complex **2**. The Ru^{II} centers are octahedral, *cis*-coordinated to two thiolate/selenolate ligands. The ruthenium center is also bound to two 1,10-phenanthroline ligands making the metal compound chiral, but because of the centrosymmetric space group both enantiomers are present in the crystal lattice. The Ni– $\text{S}_{\text{thiolate}}$ and Ni– $\text{S}_{\text{thioether}}$ distances in complex **1** are quite similar, but obviously the Ni– $\text{Se}_{\text{selenolate}}$ distances in complex **2**



Scheme 1. Synthesis scheme of the complexes $[\{\text{Ni}(\text{x}b\text{SmS})\}_2\text{Ru}(\text{phen})_2](\text{PF}_6)_2$ (**1**) and $[\{\text{Ni}(\text{x}b\text{SmSe})\}_2\text{Ru}(\text{phen})_2](\text{PF}_6)_2$ (**2**).

are longer than the Ni–S_{thioether} distances due to the larger radius of the selenium donor atom. The Ni–Ru distances are 3.72–3.77 Å in complex **1** and significantly longer (3.92–3.98 Å) in complex **2**.

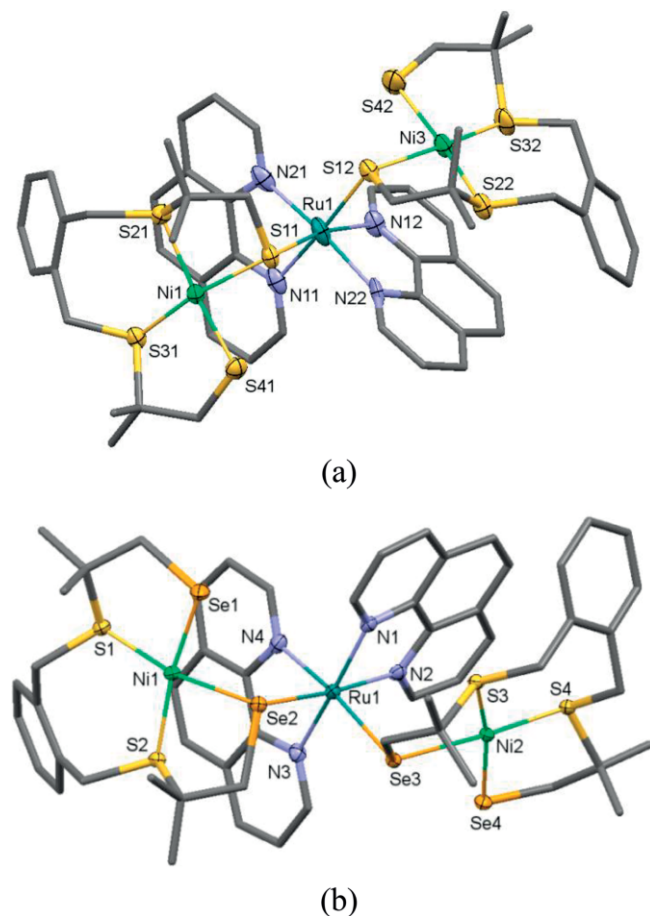


Figure 1. The molecular structures of the trinuclear dication in (a) $[(\text{Ni}(\text{xbsmS}))_2\text{Ru}(\text{phen})_2](\text{PF}_6)_2$ and (b) $[(\text{Ni}(\text{xbsmSe}))_2\text{Ru}(\text{phen})_2](\text{PF}_6)_2$ at 110(2) K. Displacement ellipsoids (50 % probability level) are shown for the atoms belonging to the first coordination spheres around the Ni and Ru centers. Hydrogen atoms, PF_6^- anions, lattice solvent molecules, and disorder are omitted for clarity.

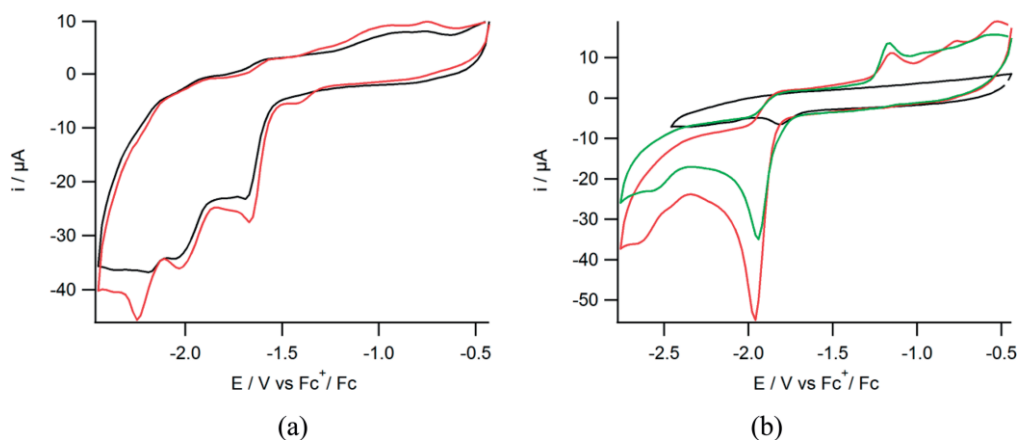


Figure 2. Cyclic voltammograms of 1 mM solutions of (a) compound **1** (black) and compound **2** (red), (b) *cis*-[Ru(phen)₂Cl₂] (black), [Ni(xbSmS)] (red), [Ni(xbSmSe)] (green) in acetonitrile containing TBAPF₆ (0.1 M) as the supporting electrolyte and a glassy carbon working electrode at 200 mV s⁻¹.

Table 1. Selected bond lengths [Å] and angles [°] for the complexes **1** and **2**.

Distances [Å]	1	Distances [Å]	2
Ni1–S11	2.2172(8)	Ni1–Se2	2.3295(5)
Ni1–S21	2.1913(8)	Ni1–S2	2.1970(9)
Ni1–S31	2.1677(8)	Ni1–S1	2.1728(9)
Ni1–S41	2.1669(9)	Ni1–Se1	2.2920(5)
Ni3–S12	2.229(6)	Ni2–Se3	2.3308(5)
Ni3–S22	2.196(6)	Ni2–S3	2.1890(9)
Ni3–S32	2.176(7)	Ni2–S4	2.1821(8)
Ni3–S42	2.172(7)	Ni2–Se4	2.2852(5)
Ru1–S11	2.3898(6)	Ru1–Se2	2.4997(4)
Ru1–S12	2.319(7)	Ru1–Se3	2.5124(4)
Ru1–N11	2.077(2)	Ru1–N4	2.065(3)
Ru1–N12	2.094(5)	Ru1–N2	2.075(3)
Angles [°]	1	Angles [°]	2
S11–Ni1–S41	84.84(3)	Se2–Ni1–Se1	82.506(17)
S11–Ni1–S21	85.83(3)	Se2–Ni1–S2	86.15(3)
S31–Ni1–S41	88.90(3)	S1–Ni1–Se1	88.65(3)
S21–Ni1–S31	102.98(3)	S2–Ni1–S1	103.50(3)
S11–Ni1–S41	84.84(3)	Se2–Ni1–Se1	82.506(17)
S11–Ni1–S21	85.83(3)	Se2–Ni1–S2	86.15(3)
S31–Ni1–S41	88.90(3)	S1–Ni1–Se1	88.65(3)
S21–Ni1–S31	102.98(3)	S2–Ni1–S1	103.50(3)
N11–Ru1–N21	79.59(11)	N4–Ru1–N3	79.58(11)
N12–Ru1–N22	77.2(3)	N2–Ru1–N1	79.46(10)
N12–Ru1–S11	167.9(2)	N2–Ru1–Se2	172.71(8)
N11–Ru1–S12	175.14(17)	N4–Ru1–Se3	173.27(8)
S11–Ru1–S12	90.80(15)	Se2–Ru1–Se3	88.969(13)

Electrochemical Analyses

The cyclic voltammograms of the [Ni₂Ru] complexes were recorded in an acetonitrile solution with tetrabutylammonium hexafluorophosphate (0.1 M) as the supporting electrolyte with a scan rate of 200 mV s⁻¹. A glassy carbon electrode was used as a working electrode, and Ag/AgCl was used as a reference electrode. All potentials are reported vs. the ferrocene/ferrocinium (Fc^{0/+}) couple ($E_{1/2} = 0.43$ V vs. Ag/AgCl). For both compounds **1** and **2** three irreversible reduction waves were observed with E_{pc} at –1.69, –2.05, and –2.19 V vs. Fc^{+/Fc} for complex **1** and at –1.68, –2.04, –2.26 V vs. Fc^{+/Fc} for complex **2** [Figure 2(a)]. The cyclic voltammograms of the mononuclear

nickel complexes show one irreversible wave with E_{pc} at -1.96 V and -1.93 V vs. Fc/Fc^+ for the compounds $[Ni(xbSmS)]$ and $[Ni(xbSmSe)]$, respectively [Figure 2(b)]. The cyclic voltammogram of *cis*- $[Ru(phen)_2(Cl)_2]$ only shows a very small reduction event, indicating that the Ru^I oxidation state is not really accessible [Figure 2(b)]. The first reduction wave for the compounds **1** and **2**, of which the peak current – compared to the second and third reduction processes – seems to indicate that two electrons are transferred, might be assigned to the reduction of two Ni^{II} centers to Ni^I . The apparent 0.3 V shift in the reduction potential of the nickel centers might be explained by the coordination of the dicationic ruthenium complex, the overall positive charge of the trinuclear compound making the Ni center more readily reduced.

Electrocatalytic Hydrogen Evolution in the Presence of HOAc

The activity of the new $[Ni_2Ru]$ compounds in electrocatalytic proton reduction was studied using cyclic voltammetry by the addition of varying amounts of HOAc to acetonitrile solutions. Both complexes show electrocatalytic activity with a peak potential around -2.1 V vs. Fc^+/Fc , as is clear from the increasing catalytic current that appears with the addition of higher amounts of acid (Figure 3). The potential at which proton reduction occurs, becomes slightly more negative at higher concentrations of acid. The overpotential for electrocatalytic proton reduction at an acetic acid concentration of 10 mM of the complexes **1** and **2** has been calculated using the half-wave potentials of the catalytic peaks, taking homoconjugation of the acid into account.^[18] Both complexes display quite similar overpotentials, which are 640 mV for complex **1** and 650 mV for complex **2**. In order to confirm that indeed dihydrogen gas is formed in the catalytic reaction, controlled-potential coulometry (CPC) experiments were carried out using 0.5 mM solutions of complexes **1** and **2** in acetonitrile (5 mL) in the presence of 10.5 μ L of HOAc (30 equiv. of H^+ per Ni_2Ru compound) at -2.1 V

vs. Fc^+/Fc . The quantification of produced dihydrogen gas was done volumetrically by GC analysis. The CPC experiment was run for 1 h, while the solution was stirred continuously. Using complex **1** as the electrocatalyst for proton reduction, a total of 49 μ L (2 μ mol) H_2 was produced per 0.5 mM complex in 1 h with 64 % faradaic yield, whereas for complex **2** a total of 56 μ L (2.3 μ mol) H_2 was produced per 0.5 mM complex in 1 h with 63 % faradaic yield. In a control experiment in the absence of the catalyst the formation of H_2 was not observed at this potential.

Discussion

In this work the compounds $[Ni(xbSmS)_2Ru(phen)_2](PF_6)_2$ (**1**) and $[Ni(xbSmSe)_2Ru(phen)_2](PF_6)_2$ (**2**) were prepared as functional mimics of the $[NiFe]$ and $[NiFeSe]$ hydrogenase active sites. X-ray crystallography showed that the trinuclear complex cations in **1** and **2** contain two square-planar nickel centers bound in *cis* positions to the octahedral ruthenium ion through a bridging thiolate or selenolate donor atom. Unexpectedly, the electrochemical properties of the two $[Ni_2Ru]$ complexes are highly similar. The substitution of the thiolate donor by a selenolate donor atom does not have a significant effect on the structure or the electrocatalytic activity. The irreversibility of the reduction processes give rise to the question as to whether the structures are stable during catalysis. The cyclic voltammograms of the parent mononuclear nickel and ruthenium complexes are different from those of the trinuclear $[Ni_2Ru]$ complexes, which might indicate that dissociation of the trinuclear $[NiRu]$ compounds in solution does not occur, but as some of the peaks seem similar to those of the parent compounds dissociation of the trinuclear structure in solution cannot be ruled out. However, the cyclic voltammograms of both $[Ni_2Ru]$ compounds show changes after the first scan (Figures S1 and S2), which might be a result of partial decomposition. Nevertheless, more studies should be done to gain insight concerning the electrocatalytic mechanism and active species in proton reduction.

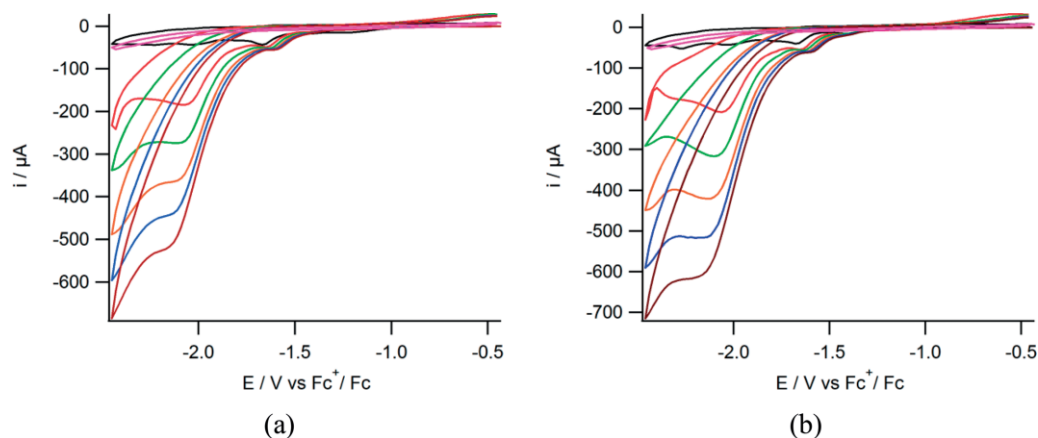


Figure 3. Cyclic voltammograms of 1 mM solutions of (a) compound **1** and (b) compound **2** in acetonitrile containing $TBAPF_6$ (0.1 M) using a glassy carbon working electrode at 200 $mV s^{-1}$ in the presence of 0 (black), 10 (red), 20 (green), 30 (orange), 40 (blue), 50 (brown) mM acetic acid and a blank with 50 mM acetic acid (pink).

Conclusions

Two new trinuclear compounds $[\{\text{Ni}(\text{xbSmS})\}_2\text{Ru}(\text{phen})_2](\text{PF}_6)_2$ and $[\{\text{Ni}(\text{xbSmSe})\}_2\text{Ru}(\text{phen})_2](\text{PF}_6)_2$ were synthesized with nickel complexes of tetradentate dithiolate and diselenolate ligands, respectively, acting as monodentate ligands to *cis*-octahedral ruthenium(II) ions. The aim of our research was to synthesize dinuclear NiRu complexes with bidentate binding of metallochalcogenate ligands, but trinuclear compounds were obtained instead. Both complexes are air-stable and in the presence of acetic acid catalyze the hydrogen evolution reaction as shown by CV and CPC experiments. However, the compounds are quite inefficient electrocatalysts for proton reduction with only very low TONs (<1 in 1 h). Unexpectedly, changing the thiolate donor atom to selenolate does not make a significant difference in the reduction potentials and electrocatalytic activity of the resulting compounds.

Experimental Section

General: All experiments were performed using standard Schlenk techniques under nitrogen unless otherwise noted. Chemicals were purchased from Acros or Aldrich and were used without further purification. Organic solvents were deoxygenated by the freeze-pump-thaw method and were dried with molecular sieves prior to use. NMR spectra were recorded with a 300 MHz Bruker DPX 300 spectrometer, and chemical shifts were referenced against the solvent peak. Mass spectra were obtained with a Finnigan TSQ-quantum instrument using ESI. Elemental analyses were performed by the Microanalytical Laboratory Kolbe in Germany. Electrochemical measurements were performed at room temperature under argon using an Autolab PGstat10 potentiostat controlled by GPES4 software. A three-electrode cell system was used with a glassy carbon working electrode, a platinum counter electrode and an Ag/AgCl reference electrode. All electrochemistry measurements were done in acetonitrile solution with tetrabutylammonium hexafluorophosphate as the supporting electrolyte; after each run ferrocene was added as an internal reference. All potentials are referenced to the half-wave potential of the redox couple of Fc^+/Fc , which under these conditions was found at 0.43 V vs. Ag/AgCl in acetonitrile, with a ΔE of 99 mV. Controlled-potential coulometry (CPC) experiments were done with the same three-electrode cell system and electrodes. CPC experiments were recorded with an Autolab PGstat10 potentiostat controlled by GPES4 software. Gas chromatographic analysis was performed with a Shimadzu gas chromatograph GC-2010 fitted with a Supelco Carboxen 1010 molecular sieves column at 35 °C. Helium was used as the carrier gas, and analytes were detected using a thermal conductivity detector operated at 80 mA. The total volume of H_2 produced during the reaction was calculated using a calibration line (Figure S3), which was obtained using the external reference method by injection of known amounts of H_2 into the GC using a Hamilton gas-tight syringe. A solution of complex **1** or **2** in acetonitrile (5 mL, 0.5 mM) was placed into a three-electrode cell, and prior to each measurement the system was de-aerated by bubbling with helium gas for 10 min. The system was closed, and the headspace was pumped through the solution for 1 min. Before each GC sampling the headspace pumping was temporarily stopped to allow equilibration of the pressure and then the GC measurement was started with a 0.5 mL sample of the headspace injection. The GC valve and the pump (KNF NMS 010 L micro diaphragm pump) were enclosed in a helium-purged housing to prevent air leaking into the system.

Single-Crystal X-ray Crystallography: All reflection intensities were measured at 110(2) K using a SuperNova diffractometer (equipped with Atlas detector) with $\text{Cu-K}\alpha$ radiation ($\lambda = 1.54178 \text{ \AA}$) for complex **1** and $\text{Mo-K}\alpha$ radiation ($\lambda = 0.71073 \text{ \AA}$) for complex **2** with the program CrysAlisPro (Version 1.171.36.32 Agilent Technologies, 2013). The same program was used to refine the cell dimensions and for data reduction. The structure was solved with the program SHELXS-2014/7 and was refined on F^2 with SHELXL-2014/7.^[19] An analytical numeric absorption correction using a multifaceted crystal model was applied using CrysAlisPro. The temperature of the data collection was controlled using the system Cryojet (manufactured by Oxford Instruments). The H-atoms were placed at calculated positions using the instructions AFIX 23, AFIX 43, or AFIX 137 with isotropic displacement parameters having values of 1.2 or 1.5 U_{eq} for the attached C-atoms. Both structures are partly disordered. CCDC 1566013 (for **1**), and 1566014 (for **2**) contain the supplementary crystallographic data for this paper. These data can be obtained free of charge from The Cambridge Crystallographic Data Centre.

Additional Notes on the Structure Determinations. 1: One of the two Ni complexes and one phenanthroline ligand coordinated to Ru are disordered over two orientations. The occupancy factors of the major components of the disorder refine to 0.543(12) and 0.550(6), respectively. The two PF_6^- counterions are found to be disordered over two orientations. The occupancy factors of the major components of the disorder refine to 0.683(4) and 0.695(4). The asymmetric unit contains 1.437 lattice acetone molecules. All solvent molecules are disordered over two orientations, but one of the two crystallographically independent solvent molecules is found at a special position. **2:** The two PF_6^- counterions are disordered over two or three orientations. All occupancy factors can be retrieved from the crystallographic information file. The crystal lattice contains some lattice acetone solvent molecules. In the asymmetric unit, there is one ordered acetone molecule [with an occupancy factor refining to 0.887(5)] and another acetone molecule disordered over an inversion center (and thus its occupancy factor was constrained to be 0.5).

Synthesis of $[\{\text{Ni}(\text{xbSmS})\}_2\text{Ru}(\text{phen})_2](\text{PF}_6)_2$: *cis*- $[\text{Ru}(\text{phen})_2(\text{Cl})_2]$ (0.119 g, 0.223 mmol) was dissolved in ethanol (8 mL), and the solution was refluxed for 2 h. This solution was transferred, with a cannula, to a Schlenk flask containing $[\text{Ni}(\text{xbSmS})]$ (0.180 g, 0.446 mmol), and the resulting reaction mixture was refluxed for 24 h. After the reaction, NH_4PF_6 (0.081 g, 0.496 mmol) was added to the hot ethanolic reaction mixture, and the solution was stirred for 30 min, resulting in a dark reddish-brown solid. The solid was collected by filtration in a yield of 0.155 g (0.097 mmol, 43 %). ^1H NMR [300 MHz, $(\text{CD}_3)_2\text{CO}$]: $\delta = 10.29$ (d, Py-H), 8.71–7.17 (aromatic region), 4.12 (d, $\text{CH}_2\text{-S21/31}$), 4.03 (d, $\text{CH}_2\text{-S22/32}$), 2.33 (d, C- $\text{CH}_2\text{-S11/41}$), 1.64 (d, C- $\text{CH}_2\text{-S12/42}$), 1.47 (t, CH_3) ppm. ESI-MS (MeCN): calcd. for $[\text{M} - 2 \text{PF}_6]^{2+}$ 633.03; found 633.7. $\text{C}_{56}\text{H}_{64}\text{F}_{12}\text{N}_4\text{Ni}_2\text{P}_2\text{RuS}_8$ (1558.04): calcd. C 43.17, H 4.14, N 3.60; found C 43.48, H 4.28, N 3.48.

Synthesis of $[\{\text{Ni}(\text{xbSmSe})\}_2\text{Ru}(\text{phen})_2](\text{PF}_6)_2$: *cis*- $[\text{Ru}(\text{phen})_2(\text{Cl})_2]$ (0.119 g, 0.223 mmol) was dissolved in ethanol (8 mL) and the solution was refluxed for 2 h. This solution was transferred, with a cannula, to a Schlenk flask containing $[\text{Ni}(\text{xbSmSe})]$ (0.222 g, 0.446 mmol), and the resulting reaction mixture was refluxed for 24 h. Then NH_4PF_6 (0.081 g, 0.496 mmol) was added while the reaction mixture was still hot, and the solution was stirred for 30 min. After filtration, a dark reddish-brown solid was obtained in a yield of 0.180 g (0.103 mmol, 46 %). ^1H NMR [300 MHz, $(\text{CD}_3)_2\text{CO}$]: $\delta = 10.22$ (d, Py-H), 8.66–7.22 (aromatic region), 4.18 (d, $\text{CH}_2\text{-S1/2}$),

4.07 (d, CH₂-S3/4), 2.53 (d, C-CH₂-Se1/2), 1.65 (d, C-CH₂-Se3/4), 1.50 (t, CH₃) ppm. ESI-MS (MeCN): calcd. for [M - 2 PF₆]²⁺ 727.2; found 727.2. C₅₆H₆₄F₁₂N₄Ni₂P₂RuS₄Se₄·0.3C₃H₆O: calcd. C 38.86, H 3.79, N 3.16; found C 39.12, H 3.90, N 3.08.

Acknowledgments

We thank Dr. D. G. H. Hetterscheid for helpful discussions. Mr. J. J. M. van Brussel and Mr. W. Jesse are gratefully acknowledged for performing the ESI-MS measurements.

Keywords: Hydrogenases · Ni₂Ru complexes · Electrocatalysis · Cyclic voltammetry · Proton reduction · Selenium · Sulfur

- [1] C. Tard, C. J. Pickett, *Chem. Rev.* **2009**, *109*, 2245–2274.
 [2] M. T. M. Koper, E. Bouwman, *Angew. Chem. Int. Ed.* **2010**, *49*, 3723–3725; *Angew. Chem.* **2010**, *122*, 3810.
 [3] M. Stephenson, L. H. Stickland, *Biochem. J.* **1931**, *25*, 205–214.
 [4] W. Lubitz, H. Ogata, O. Rüdiger, E. Reijerse, *Chem. Rev.* **2014**, *114*, 4081–4148.
 [5] G. M. Chambers, M. T. Huynh, Y. Li, S. Hammes-Schiffer, T. B. Rauchfuss, E. Reijerse, W. Lubitz, *Inorg. Chem.* **2016**, *55*, 419–431.
 [6] T. R. Simmons, G. Berggren, M. Bacchi, M. Fontecave, V. Artero, *Coord. Chem. Rev.* **2014**, *271*, 127–150.
 [7] S. Canaguier, M. Fontecave, V. Artero, *Eur. J. Inorg. Chem.* **2011**, 1094–1099.
 [8] S. Canaguier, L. Vaccaro, V. Artero, R. Ostermann, J. Pécaut, M. J. Field, M. Fontecave, *Chem. Eur. J.* **2009**, *15*, 9350–9364.
 [9] Y. Oudart, V. Artero, L. Norel, C. Train, J. Pécaut, M. Fontecave, *J. Organomet. Chem.* **2009**, *694*, 2866–2869.
 [10] Y. Oudart, V. Artero, J. Pécaut, C. Lebrun, M. Fontecave, *Eur. J. Inorg. Chem.* **2007**, 2613–2626.
 [11] G. M. Chambers, R. Angamuthu, D. L. Gray, T. B. Rauchfuss, *Organometallics* **2013**, *32*, 6324–6329.
 [12] E. Garcin, X. Venede, E. Hatchikian, A. Volbeda, M. Frey, J. Fontecilla-Camps, *Structure* **1999**, *7*, 557–566.
 [13] C. Wombwell, E. Reisner, *Chem. Eur. J.* **2015**, *21*, 8096–8104.
 [14] G. Gezer, D. Durán Jiménez, M. A. Siegler, E. Bouwman, *Dalton Trans.* **2017**, *46*, 7506–7514.
 [15] J. A. Verhagen, D. D. Ellis, M. Lutz, A. L. Spek, E. Bouwman, *J. Chem. Soc., Dalton Trans.* **2002**, 1275–1280.
 [16] J. E. Collins, J. J. S. Lamba, J. C. Love, J. E. McAlvin, N. Christina, B. P. Peters, W. Xufeng, C. L. Fraser, *Inorg. Chem.* **1999**, *38*, 2020–2024.
 [17] D. Steinmann, T. Nauser, W. H. Koppenol, *J. Org. Chem.* **2010**, *75*, 6696–6699.
 [18] V. Fourmond, P. A. Jacques, M. Fontecave, V. Artero, *Inorg. Chem.* **2010**, *49*, 10338–10347.
 [19] G. M. Sheldrick, *Acta Crystallogr., Sect. C* **2015**, *71*, 3–8.

Received: August 3, 2017